Reproducibility and transferability of topological data: experimental charge density study of two modifications of L-alanyl-L-tyrosyl-L-alanine†

Lilianna Chęcińska,[a,b,d] Stefan Mebs,[b] Christian B. Hübschle,[b] Diana Förster,[b] Wolfgang Morgenroth[c,e,f] and Peter Luger*[b]

Received 31st May 2006, Accepted 5th July 2006
First published as an Advance Article on the web 2nd August 2006
DOI: 10.1039/b607744g

Two crystalline modifications of the tripeptide L-Ala–L-Tyr–L-Ala, which have different solvent molecules in the crystal structure (water and ethanol for modifications **1** and **2**), were the subject of experimental charge density studies based on high resolution X-ray data collected at ultra-low temperatures of 9 K (**1**) and 20 K (**2**), respectively. The molecular structures and the intermolecular interactions were found to be rather similar in the two crystal lattices, so that this study allowed the reproducibility of the charge density of a given molecule in different (but widely comparable) crystalline environments to be examined. With respect to bond topological and atomic properties, the agreement between the two modifications of the title tripeptide was in the same range as found from the comparison with the previously reported results of tri-L-alanine. It follows that the reproducibility and transferability of quantitative topological data are comparable and that within the accuracy of experimental charge density work the replacement of the central amino acid residue L-Ala by L-Tyr has no significant influence, neither on bond nor on the atomic properties of the oligopeptide main chain. Intermolecular interactions in the form of hydrogen bonds were characterized quantitatively and qualitatively by topological criteria and by mapping the charge density distribution on the Hirshfeld surface.

Introduction

Thanks to the technical developments of recent years, the time consuming nature of high resolution X-ray diffraction experiments has been reduced significantly, so that experimental charge density determinations on entire classes of chemically-related compounds or on larger molecules can be carried out in a reasonable time.[1,2] Almost at the same time, computational and theoretical developments have taken place allowing the quantitative properties of a chemical system to be determined. Especially, Bader's quantum theory of atoms in molecules (QTAIM)[3] allows the derivation of bonding, non bonding and atomic properties from the topological analysis of a charge density distribution $\rho(\mathbf{r})$. One key concept of Bader's theory is the transferability of submolecular or atomic electronic properties providing a tool to enter these fragments as building blocks for the additive generation of electron densities of macromolecules, like proteins or oligonucleotides, which are otherwise obtainable only in exceptional cases. Since the transferability concept is essential for the application of database approaches to model the electron density of larger systems, its experimental verification is of major importance. In the class of the 20 genetically encoded amino acids, the so-far experimentally-derived topological properties of 16 of the 20 compounds can serve for that purpose.[4–10] They have, in addition, been completed by theoretical calculations by Matta & Bader for all 20 amino acids in their neutral forms.[11–13]

The measure of transferability has to be seen in the light of the reproducibility of topological quantities obtained from an experimental charge density study. We have studied this aspect in two cases, once by two high resolution data collections on a hexapeptide under different experimental conditions[14] and in another study on strychnine where we compared topological results based on four data sets taken at different temperatures and with different experimental setups.[15] The general finding in all cases was that transferability and reproducibility was confirmed, for example, for the electron densities $\rho(\mathbf{r}_{BCP})$ and the Laplacians $\nabla^2\rho(\mathbf{r}_{BCP})$ at the bond critical points $\mathbf{r}_{BCP}$ (defined by the condition that the gradient $\nabla\rho(\mathbf{r})$ vanishes at $\mathbf{r}_{BCP}$) within 0.1 eÅ^{-3} and 3–4 eÅ^{-5}, respectively.

For an experimental verification of transferability also in the oligopeptide field, we entered into comparative charge density studies of tripeptides of the type L-Ala–XXX–L-Ala, where XXX was to be varied among the 20 naturally occurring amino acids. A corresponding study of the reference tripeptide L-Ala–L-Ala–L-Ala (tri-L-alanine, **3**) has been published recently.[16] Here we present as a second example a comparison of the experimental charge

[a]*Department of Crystallography and Crystal Chemistry, University of Łódź, Pomorska 149/153, 90 236, Łódź, Poland*
[b]*Institute for Chemistry and Biochemistry/Crystallography, Free University Berlin, Fabeckstr. 36a, 14 195, Berlin, Germany. E-mail: luger@chemie.fu-berlin.de*
[c]*Department of Chemistry, Aarhus University, Langelandsgade 140, 8000, Aarhus C, Denmark*
[d]*Institute for Chemistry and Biochemistry/Crystallography, Free University Berlin, Takustr. 6, 14 195, Berlin, Germany*
[e]*Institute for Inorganic Chemistry, Georg August University, Tammannstr. 4, 37 077, Göttingen, Germany*
[f]*c/o DESY/HASYLAB, Notkestr. 85, 22 603, Hamburg, Germany*
† Electronic supplementary information (ESI) available: Table of non-bonded valence shell charge concentrations, VSCCs. See DOI: 10.1039/b607744g

densities of two modifications of L-Ala–L-Tyr–L-Ala with different solvent molecules in the crystal lattice, water for modification **1** and ethanol for modification **2**.

From the conventional spherical structure analyses[17] it was found that the molecular structures in the two modifications were very similar and that even the intermolecular interactions in terms of hydrogen bonds were, in most cases, comparable with only few exceptions in the contacts to the different solvent molecules. Hence, this study represents a favorable case where the reproducibility of the charge density of a given molecule in different crystal structures but widely comparable crystalline environment can be studied more so, since also the experimental conditions (see the Experimental section) are different. In addition, concerning transferability, the atomic and bond topological properties of the main peptide chain can be compared to the corresponding values of tri-L-alanine.

Results and discussion

Charge density and bond topological analysis

The molecular structures with atom-numbering schemes of both investigated modifications of L-Ala–L-Tyr–L-Ala (**1** and **2**) are shown in Fig. 1a–b. Modification **1** consists of one tripeptide molecule and an average of 2.6 water molecules (1 + 1 + 0.6) in the asymmetric unit. For the second one, the solvent is represented by one ethanol molecule. The molecular structures and crystal packings were well discussed before.[17] The agreement in bond lengths and further geometric properties between the present high-order multipole refinements and previous low-order spherical refinements is in the range of 3σ, hence no detailed discussion is needed.

To get a quantitative description of the electronic structures of **1** and **2** full topological analyses were carried out with the XDPROP program of the XD program package.[18] The bond topological properties in terms of $\rho(\mathbf{r}_{BCP})$ and $\nabla^2\rho(\mathbf{r}_{BCP})$ values for the 15 main chain bonds are summarized in Table 1 together with the corresponding properties of **3**.

The electron densities $\rho(\mathbf{r}_{BCP})$ of all 23 non-hydrogen bonds differ between **1** and **2** within an average of 0.07 eÅ^{-3} whereas the Laplacians $\nabla^2\rho(\mathbf{r}_{BCP})$ differ by 4.9 eÅ^{-5}. As already mentioned comparable discrepancies were reported in the literature for averages from experimental studies in the peptide field and also for the results obtained from different data sets of one compound. In our study on strychnine[15] two data sets were measured at comparable experimental conditions as in the present case (synchrotron and Mo Kα primary radiation, T ~10–20 K). The average differences in $\rho(\mathbf{r}_{BCP})$ and $\nabla^2\rho(\mathbf{r}_{BCP})$ were 0.07 eÅ^{-3} and 2.7 eÅ^{-5}, respectively. Similar results were also obtained for the above mentioned hexapeptide. While in these cases the same crystal lattice was subject to electron density determinations at different experimental conditions, the present study provides bond topological data of a given compound in two crystal lattices where, however, the intermolecular environments are rather alike. Hence average spreads in the range of 0.1 eÅ^{-3} and 3–5 eÅ^{-5} seem to indicate the reproducibility of these quantities from charge density determinations at different experimental conditions and even in different crystal lattices if the intermolecular interactions are comparable.

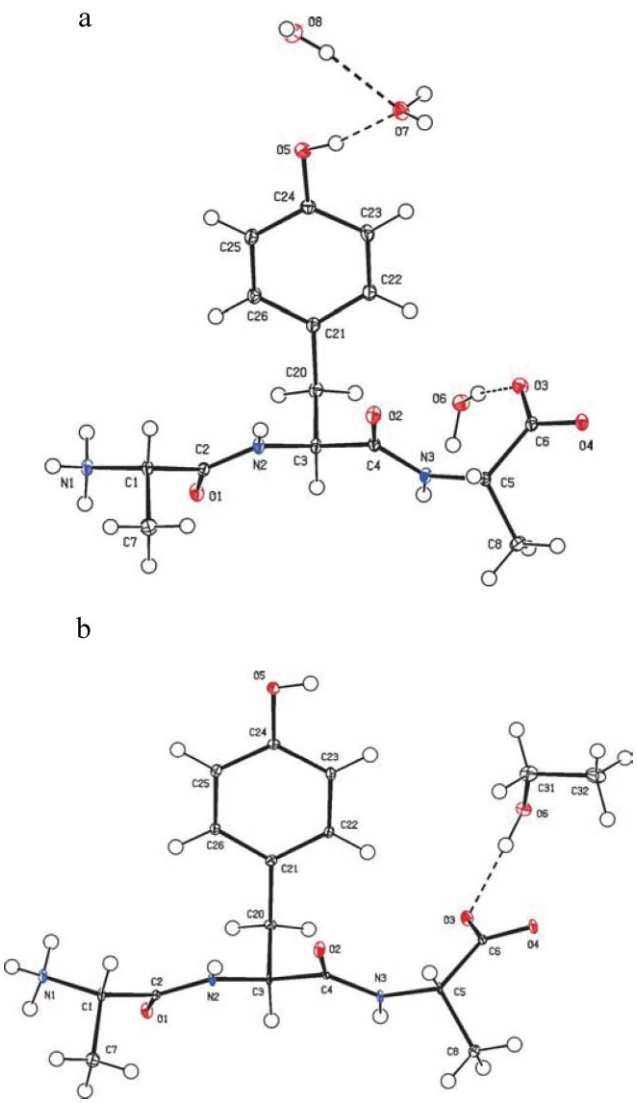

Fig. 1 Molecular structures of **1** at 9 K (a) and **2** at 20 K (b) with the chosen atom-numbering scheme. Displacement ellipsoids are drawn at a 50% probability level and H atoms are shown as small spheres of arbitrary radii.[42]

It is interesting to note that a comparable spread is also seen if experimental and theoretical values for $\rho(\mathbf{r}_{BCP})$ and $\nabla^2\rho(\mathbf{r}_{BCP})$ are compared, see corresponding results of a B3LYP/6-311 + + G(3df,3pd) calculation at experimental geometry, listed also in Table 1. The agreement between the experimental averages of **1** and **2** and theory for the 15 main chain bonds in Table 1 is 0.12 eÅ^{-3} and 6.4 eÅ^{-5}, respectively. Noticeable differences exist for the Laplacians of the polar C–O bonds, which are significantly stronger negative experimentally compared to theory. This is a general finding, even positive theoretical Laplacians are reported in the literature for C–O bonds.[13] The limited flexibility of the radial functions is considered responsible for such observed discrepancies.[19] For the remaining 11 non C–O bonds the experimental/theoretical differences reduce to 0.08 eÅ^{-3} and 3.7 eÅ^{-5}, so that in total the experimental and theoretical bond topological properties can be regarded reliable in these ranges.

Table 1 Bond topological properties $\rho(\mathbf{r}_{BCP})$ and $\nabla^2\rho(\mathbf{r}_{BCP})$ of comparable bonds for L-Ala–L-Tyr–L-Ala (**1** and **2**) and L-Ala–L-Ala–L-Ala (**3**) (in eÅ^{-3} and eÅ^{-5}). The types of the neighbour atoms not directly involved in the bond are given in brackets. For the title compound the first and second lines refer to modifications **1** and **2**;for **3** they refer to the two crystallographically independent molecules

Bond type	Bond	Experimental **1**/**2** $\rho(\mathbf{r})$	Theoretical **1**/**2** $\rho(\mathbf{r})$	Experimental **3** $\rho(\mathbf{r})$	Experimental **1**/**2** $\nabla^2\rho(\mathbf{r})$	Theoretical **1**/**2** $\nabla^2\rho(\mathbf{r})$	Experimental **3** $\nabla^2\rho(\mathbf{r})$
N_{amm}–C_α–[C_{pep}]	N(1)–C(1)	1.70(3)	1.59	1.83(4)	−8.9(1)	−13.2	−14.2(2)
		1.71(3)		1.69(4)	−9.3(1)		−8.3(2)
N_{pep}–C_{pep}–[C_α–N_{amm}]	N(2)–C(2)	2.44(4)	2.32	2.39(4)	−20.6(2)	−26.3	−23.3(2)
		2.43(3)		2.43(4)	−24.4(2)		−21.9(2)
[C_{carbox}–C_α]–N_{pep}–C_{pep}	N(3)–C(4)	2.39(4)	2.31	2.43(4)	−19.2(2)	−26.1	−22.0(2)
		2.53(3)		2.45(4)	−27.0(2)		−24.8(2)
N_{pep}–C_α–[C_{pep}]	N(2)–C(3)	1.75(3)	1.72	1.82(4)	−9.4(1)	−15.8	−9.4(2)
		1.84(3)		1.88(4)	−12.5(1)		−13.2(2)
N_{pep}–C_α–[C_{carbox}]	N(3)–C(5)	1.81(3)	1.71	1.80(4)	−9.6(1)	−15.3	−10.7(2)
		1.88(3)		1.80(4)	−14.4(1)		−10.9(2)
[N_{amm}]–C_α–C_{pep}	C(1)–C(2)	1.67(3)	1.72	1.74(4)	−8.9(1)	−15.2	−11.3(2)
		1.75(3)		1.76(4)	−13.6(1)		−11.7(2)
[N_{pep}]–C_α–C_{pep}	C(3)–C(4)	1.64(3)	1.71	1.64(4)	−7.8(1)	−15.0	−9.0(2)
		1.76(3)		1.72(4)	−12.9(1)		−13.1(2)
[N_{amm}]–C_α–C_β	C(1)–C(7)	1.71(3)	1.64	1.59(4)	−9.9(1)	−13.6	−8.4(2)
		1.79(3)		1.61(4)	−13.7(1)		−9.4(2)
[C_{carbox}]–C_α–C_β	C(5)–C(8)	1.60(3)	1.62	1.59(4)	−8.3(1)	−13.3	−9.0(2)
		1.68(3)		1.61(4)	−10.9(1)		−10.2(1)
[N_{pep}]–C_α–C_β	C(3)–C(20)	1.61(3)	1.55	1.58(4)	−7.3(1)	−11.9	−7.2(1)
		1.63(3)		1.62(3)	−10.9(1)		−10.0(1)
[N_{pep}]–C_α–C_{carbox}	C(5)–C(6)	1.59(3)	1.67	1.79(4)	−6.7(1)	−14.2	−11.5(2)
		1.77(3)		1.77(4)	−14.2(1)		−10.9(2)
O_{carbox}–C_{carbox} [shorter]	O(3)–C(6)	2.97(4)	2.61	2.82(5)	−34.5(3)	−17.1	−32.6(3)
		2.81(4)		2.82(5)	−30.1(3)		−33.5(3)
O_{carbox}–C_{carbox} [longer]	O(4)–C(6)	2.64(4)	2.51	2.76(5)	−24.1(2)	−21.8	−30.6(3)
		2.75(4)		2.67(5)	−34.7(2)		−25.3(3)
O_{pep}–C_{pep}–[C_α–N_{amm}]	O(1)–C(2)	2.95(4)	2.72	2.92(5)	−25.6(2)	−17.3	−30.4(3)
		2.83(5)		2.82(5)	−35.7(3)		−24.5(3)
O_{pep}–C_{pep}	O(2)–C(4)	2.99(4)	2.71	2.88(5)	−28.8(3)	−16.8	−32.4(3)
		2.98(5)		2.86(5)	−42.8(3)		−30.5(3)

Two peptide bonds link the three amino acid residues, being next to the N-terminus and the C-terminus, respectively. It follows from both experimental and theoretical results that comparable types of bonds (N_{pep}–C_{pep}, N_{pep}–C_α, C_α–C_{pep}, O_{pep}–C_{pep}) are characterized by a similar topology disregarding the different neighbour groups. Hence a next nearest neighbour influence is not detectable, which holds also for the C_α–C_β bond in spite of the different substituents at C_β.

Atomic properties

Following Bader's quantum theory of atoms in molecules (QTAIM) a molecule can be partitioned into submolecular fragments. The partitioning procedure to obtain atomic regions makes use of the zero-flux surfaces in the electron density gradient vector field $\nabla\rho(\mathbf{r})$. In order to evaluate the atomic volumes and charges, the algorithm available through the TOPXD program[20] was applied. The results for the main chain atoms of **1**, **2** and **3** are summarized in Table 2.

The total atomic volumes, V_{tot}, are defined by the interatomic boundaries in the crystal. It is common practise to consider also the V_{001} volumes, defined by a cutoff at $\rho = 0.001$ au, which are used to compare with theoretically obtained charge densities of isolated molecules. For both modifications, **1** and **2**, the sum of V_{tot} (multiplied by $Z = 2$) reproduces the unit cell volumes to within 1%, whereas the charges add up to zero within ±0.04 e, indicating that the partitioning procedure has worked properly.

It is interesting to note that the total volume of a single tripeptide molecule of the water modification (~388 Å^3) is smaller than the ethanol one (~412 Å^3). Detailed analysis revealed that the essential differences in the atomic volumes are observed for the methyl and ammonium groups and the oxygen atom O(5), hence the outer regions of the peptide molecules where the major intermolecular interactions take place. Based on V_{001} the above mentioned differences vanish (both ~343 Å^3). Taking into account these findings and a number of potential hydrogen bonds in both crystals, it seems that the molecules in the water modification crystal are more densely packed than in the ethanol one.

Consideration of individual atomic properties suggests the following trend:

For the nitrogens the N_{amm} atom has a slightly larger volume than the peptide nitrogens being accompanied by a somewhat more negative charge.

However, the carbons differ strongly by their atomic charges. The C_α and C_β atoms have weak positive charges, while the charges of the peptide carbons are close to +1 and the C_{carbox} carbon is even stronger positively charged. No significant differences are seen between the O_{pep} and O_{carbox} oxygens having comparable volumes and agree in charges close to −1.

As already found for the bond topological properties, the atomic properties in the peptide bond regions also do not depend on whether this region is next to the N-terminus or the C-terminus. In total the average agreement of V_{001} and Q_{001} values for the atoms listed in Table 1 for **1** and **2** is 0.8 Å^3 and 0.1 e, respectively.

Table 2 Atomic volumes (V_{tot}/Å^3 and V_{001}/Å^3) and charges (Q_{001}/e) for comparable atoms of **1**, **2** and **3** derived from the experimental charge density. The neighbour atom types are given in brackets. First and second lines defined as in Table 1

Atom type	Atom	**1/2** V_{tot}	**1/2** V_{001}	**3** V_{001}	**1/2** Q_{001}	**3** Q_{001}
N_{amm}	N(1)	17.87	16.33	13.90	−1.51	−1.12
		14.53	14.18	14.80	−1.46	−1.34
$[N_{amm}–C_{\alpha}–C_{pep}]–N_{pep}$	N(2)	13.62	12.50	12.49	−0.93	−1.04
		13.98	12.53	12.80	−1.09	−1.00
$[C_{carbox}–C_{\alpha}]–N_{pep}$	N(3)	12.59	12.15	12.58	−0.91	−1.06
		14.51	12.81	12.64	−1.03	−1.02
$[N_{amm}–C_{\alpha}]–C_{pep}$	C(2)	6.83	6.62	5.78	0.88	1.10
		7.25	6.64	5.91	1.01	1.05
$[N_{pep}–C_{\alpha}]–C_{pep}$	C(4)	7.12	6.78	6.04	0.83	1.11
		7.15	6.56	5.87	1.04	1.14
$[N_{amm}]–C_{\alpha}$	C(1)	6.75	6.69	7.34	0.24	0.07
		7.24	7.03	7.29	0.18	0.04
$[N_{pep}]–C_{\alpha}–[C_{pep}]$	C(3)	6.52	6.52	6.98	0.25	0.17
		7.47	7.25	6.77	0.09	0.27
$[C_{carbox}]–C_{\alpha}$	C(5)	7.11	6.95	7.06	0.26	0.21
		7.83	7.54	6.82	0.14	0.22
$[N_{amm}–C_{\alpha}]–C_{\beta}$	C(7)	9.29	8.82	8.90	0.19	0.25
		12.21	9.53	8.39	0.10	0.26
$[C_{carbox}–C_{\alpha}]–C_{\beta}$	C(8)	9.95	9.10	9.30	0.19	0.16
		10.72	9.67	9.28	0.10	0.13
C_{carbox}	C(6)	5.24	5.08	6.08	1.36	1.13
		6.97	6.35	5.70	1.23	1.21
$[N_{amm}–C_{\alpha}–C_{pep}]–O_{pep}$	O(1)	17.61	15.87	16.20	−1.06	−1.09
		17.65	15.65	15.92	−0.93	−1.15
$[N_{pep}–C_{\alpha}–C_{pep}]–O_{pep}$	O(2)	19.48	16.11	15.98	−0.99	−1.09
		17.48	14.38	15.97	−1.09	−1.13
O_{carbox} [shorter]	O(3)	18.46	16.00	16.46	−1.09	−1.01
		17.90	16.47	16.52	−1.04	−0.96
O_{carbox} [longer]	O(4)	16.20	14.84	15.28	−0.96	−1.03
		18.18	16.64	14.80	−1.04	−0.98

Hydrogen bond topology

An analysis of the crystal packing of both modifications of L-Ala–L-Tyr–L-Ala provided information about potential hydrogen bonds (HBs). The discussion based on the spherical structure[17] considered only steric criteria which are, for example, applied in geometry analysis programs like PLATON.[42] However, various criteria have been developed to describe HBs according to topological properties. For example, Koch & Popelier[21] have evaluated eight concerted effects occurring in the charge density, which are indicative of hydrogen bonding while Espinosa *et al.*[22] have derived exponential relations for HB energies from the analysis of experimental electron density studies, so that quantitative topological criteria allow a better insight into the strengths of these interactions. Geometrical and bond topological parameters of the possible HBs for **1** and **2** are listed in Table 3 (see the ESI for nonbonded valence shell charge concentrations (VSCCs)).

According to the topological criteria for the existence of hydrogen bonds, postulated by Koch and Popelier,[21] 11 such intermolecular interactions are found for **1** and 7 for **2**. Each of them is characterized by low values of the electron density and a positive Laplacian at the hydrogen $\cdots$ acceptor bond critical point. Moreover, a decrease of volume and a loss of charge of hydrogen atoms participating in H-bond interactions are observed.

Taking into account the geometrical (D $\cdots$ A and H $\cdots$ A distances) and topological criteria ($\rho(\mathbf{r}_{BCP})$, $\nabla^2\rho(\mathbf{r}_{BCP})$) together, the hydroxyl group of the tyrosyl fragment creates the strongest HB in both modification of L-Ala–L-Tyr–L-Ala. This observation is supported by the highest H-bond energies for these interactions ($\cong$ 60 kJ mol^{-1}). All energies presented in Table 3 are calculated with the relation given by Espinosa *et al.*, [E_{HB} = 25300 × exp(−3.6 × (H $\cdots$ A) kJ mol^{-1}]].[22] The next strong intermolecular interactions are O(6)–H(16) $\cdots$ O(3) and N(1)–H(11C) $\cdots$ O(2) for **2**, which are characterized by electron density values of 0.26 and 0.25 e Å^{-3} and their H-bond energies amount to 51.8 kJ mol^{-1}. The remaining O–H $\cdots$ O and N_{amm}–H $\cdots$ O HBs are weaker with the electron density in the range of 0.08–0.23 e Å^{-3}. The interactions of the type N_{pep}–H...O_{pep} are the weakest ones with HB energies below 20 kJ mol^{-1}. A similar observation was also made for tri-L-alanine where the four interpeptide linkages belonged to the weaker ones and there was a tendency, also seen in this study, that the stronger HBs were established to solvent molecules.

Finally, for all HBs described for both modifications of L-Ala–L-Tyr–L-Ala, the exponential correlation between electron density (or corresponding Laplacian) and the hydrogen $\cdots$ acceptor distance have been found; the correlation coefficients (R) amount to 0.90 and 0.93, respectively (Fig. 2a–b). These findings are in agreement with Espinosa's studies.[23] Moreover, a linear relationship between the electron density and H-bond energy is observed (R = 0.92), which is presented in Fig. 2c.

The site and strength of an intermolecular interaction can be made visible by means of the Hirshfeld surface[24] which is defined by the share-holder principle ρ_{mol}/ρ_{cryst} = 0.5. It is displayed in Fig. 3 for modification **2** together with the electron density mapped by a colour code on this surface. The graphics was generated with the in-house written program MOLISO.[25] Strong interactions can

Table 3 Geometric and topological parameters of the hydrogen bonds for **1** and **2** (distances in Å, angles in deg, electron density at H ⋯ *A* BCP in eÅ^{-3} and its corresponding Laplacian in e Å^{-5}, E_{HB} in kJ mol^{-1})

D–H ⋯ *A*	*D*—H	H ⋯ *A*	*D* ⋯ *A*	*D*—H ⋯ A	$\rho(\mathbf{r})$	$\nabla^2\rho(\mathbf{r})$	E_{HB}
1							
O(5)–H(15) ⋯ O(7)	0.97	1.68	2.6301(7)	167	0.21(3)	5.3(1)	59.9
O(6)–H(61) ⋯ O(3)	0.97	1.89	2.8462(8)	169	0.08(2)	3.2(1)	28.1
O(6)–H(62) ⋯ O(4)[a]	0.97	1.86	2.8208(6)	173	0.15(3)	3.4(1)	31.3
O(7)–H(71) ⋯ O(3)[b]	0.97	1.79	2.7473(6)	171	0.16(3)	4.3(1)	40.2
O(7)–H(72) ⋯ O(6)[c]	0.97	1.81	2.7702(6)	174	0.10(3)	4.2(1)	37.4
O(8)–H(81) ⋯ O(7)	0.97	1.95	2.9167	174	0.08(1)	3.2(1)	22.6
N(1)–H(11A) ⋯ O(4)[d]	1.03	1.79	2.8274(6)	177	0.17(2)	3.1(1)	40.2
N(1)–H(11B) ⋯ O(5)[e]	1.03	1.76	2.7934(5)	173	0.17(3)	4.4(1)	44.8
N(1)–H(11C) ⋯ O(2)[f]	1.03	1.85	2.8233(8)	156	0.15(2)	3.0(1)	32.4
N(2)–H(12) ⋯ O(1)[g]	1.01	2.00	2.9488(5)	156	0.07(2)	2.2(1)	18.9
N(3)–H(13) ⋯ O(4)[a]	1.01	2.04	3.0300(8)	168	0.04(2)	1.8(1)	16.4
2							
O(5)–H(15) ⋯ O(6)[a]	0.97	1.67	2.6249(6)	170	0.27(3)	5.1(1)	62.0
O(6)–H(16) ⋯ O(3)	0.97	1.72	2.6883(6)	178	0.26(3)	4.1(1)	51.8
N(1)–H(11A) ⋯ O(4)[d]	1.03	1.77	2.7844(5)	168	0.23(2)	3.4(1)	43.2
N(1)–H(11B) ⋯ O(5)[g]	1.03	1.84	2.8738(5)	174	0.18(2)	3.3(1)	33.6
N(1)–H(11C) ⋯ O(2)[h]	1.03	1.72	2.7501(7)	178	0.25(3)	3.9(1)	51.8
N(2)–H(12) ⋯ O(1)[e]	1.01	2.04	2.9773(5)	153	0.09(2)	2.0(1)	16.4
N(3)–H(13) ⋯ O(4)[b]	1.01	1.99	2.9656(8)	161	0.09(2)	2.3(1)	19.6

Symmetry codes:[a] $-x, y-1/2, 2-z$. [b] $1-x, 1/2+y, 2-z$. [c] $x, 1+y, z$. [d] $x, y, z-1$. [e] $1-x, y-1/2, 1-z$. [f] $-x, y-1/2, 1-z$. [g] $-x, 1/2+y, 1-z$. [h] $1-x, 1/2+y, 1-z$.

easily be identified in the donor regions close to H(15) and H(11A) and the acceptor region next to O(2). Further strong interactions as listed in Table 3 are on the back side of the molecule with respect to Fig. 3 and made invisible in this representation for clarity. The software used to generate this drawing allows an online rotation of this image on a graphic screen, so that all close contacts and their implications on the charge density rearrangement can be visualized and examined in three dimensions.

Electrostatic potential

The electrostatic potential (EP), which can be derived directly from the electron density, is an analytical tool which is used to predict the reactive behaviour of chemical systems and to study, for example, biological recognition processes. It was calculated from the experimental data using the method of Su & Coppens[26] and is displayed in Fig. 4 for both modifications **1** and **2**. The EP is represented by a color code (see color bars) on the iso electron density surface at $\rho = 0.5$ e Å^{-3}.

First of all it can be seen that the EP distributions on both molecular surfaces are rather alike, confirming the conservation of the electronic properties of the tripeptide in both crystal lattices. Moreover, the polarization of the electron density is visibly very pronounced in regions involved in hydrogen bonding. Donor hydrogen atoms, for example the ammonium hydrogens, the phenolic OH hydrogen of the tyrosine side group and the water hydrogens, exhibit stronger positive regions than are seen for methyl or phenyl hydrogens. The negative potential is then concentrated around the oxygen atoms, being the HB acceptor atoms

Transferability of submolecular fragments

With respect to the transferability of electronic properties of chemically equivalent atoms the topology of the main peptide chain of both modifications of L-Ala–L-Tyr–L-Ala have been compared with literature data for tri-L-alanine.[16] Considering bond topological parameters, average differences between **1**/**2** of Ala–Tyr–Ala and tri-L-alanine are 0.08/0.06 e Å^{-3} for the electron densities at the bond critical points and 2.5/3.9 e Å^{-5} for the corresponding Laplacians, respectively. Of major interest are the topological descriptors in the five important backbone bond types O_{pep}–C_{pep}, N_{pep}–C_{pep}, N_{pep}–C_{α}, C_{α}–C_{pep}, C_{α}–C_{β}. The distribution of their $\rho(\mathbf{r}_{BCP})$ and $\nabla^2\rho(\mathbf{r}_{BCP})$ values in the eight peptide bond regions (four in Ala–Tyr–Ala molecules of **1** and **2** and four in the two crystallographically independent tri-L-alanine molecules) is shown in Fig. 5. It can be seen that the spread is small for the electron density values and larger for the Laplacians, however, in no case is an influence of the central amino acid on the main chain topology seen. This is confirmed by the averages listed in Table 4, where the statistical uncertainties (0.04–0.07 e Å^{-3} and 2–6 e Å^{-5}) are in the same ranges as given above when only corresponding properties for **1** and **2** of Ala–Tyr–Ala were compared.

This transferability found for bond topological properties is supported by a comparison of atomic properties. This can be seen from individual atom volumes and charges which are listed for **1**, **2** and both independent molecules of tri-L-alanine (**3**) in Table 2, but even better from the averages summarized in Table 5. For all atoms

Table 4 Averaged values of electron density and Laplacian at the BCPs (in e Å^{-3} and e Å^{-5}, respectively) for the different bond types in **1**, **2** and **3** derived from experiment, n = no. of contributing data

Bond type	n	$\rho(\mathbf{r})$	$\nabla^2\rho(\mathbf{r})$
O_{pep}–C_{pep}	8	2.90(7)	−31.3(58)
N_{pep}–C_{pep}	8	2.44(4)	−22.9(25)
N_{pep}–C_{α}	8	1.82(4)	−11.3(19)
C_{α}–C_{pep}	8	1.71(5)	−11.0(22)
C_{α}–C_{β}	12	1.64(6)	−9.6(18)

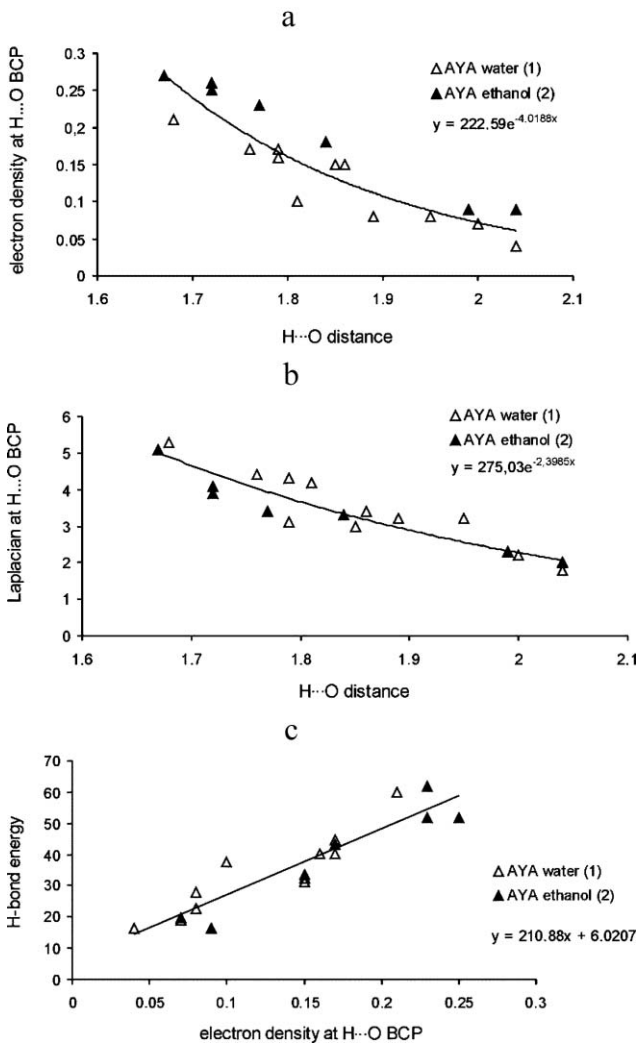

Fig. 2 Relationships of (a) $\rho(\mathbf{r}_{BCP})$ and (b) $\nabla^2\rho(\mathbf{r}_{BCP})$ at H···O bond critical points (in e Å^{-3}/e Å^{-5}) plotted *vs* H···O distances (in Å). (c) Correlation between the H-bond energy/kcal mol^{-1} and $\rho(\mathbf{r}_{BCP})$/e Å^{-3} at H···O bond critical points.

in the peptide bond region the internal consistency is within 0.1 e for the charges and 0.9 Å^3 for the volumes. Moreover the averages for the eight peptide groups in **1**, **2** and **3** compare properly with the corresponding results from a study on five dipeptides and one hexapeptide (second lines in Table 5).[27]

Table 5 Averaged charges Q_{001} (e) and volumes V_{001} (Å^3)for the atoms in the peptide groups of **1**, **2**, **3** (first line), corresponding averages from the literature[27] (second line), n = number of contributing data

Atom	n	Q_{001}	V_{001}
C_α	12	0.18(7)	7.0(3)
	16	0.24(9)	7.1(6)
C_{pep}	8	1.02(10)	6.3(4)
	11	0.98(7)	6.6(4)
O_{pep}	8	−1.07(7)	15.7(6)
	11	−0.87(10)	16.1(6)
N_{pep}	8	−1.01(6)	12.6(2)
	11	−1.00(6)	11.7(9)

Hence, neither from bond topological nor atomic properties can be seen any influence from whether the central amino acid is alanine or tyrosine. This verifies experimentally Bader's concept of the transferability of chemically equivalent submolecular fragments and encourages the use of database approaches for electron density modelling of macromolecules.[28–31]

Experimental

Two modifications of the tripeptide L-alanyl–L-tyrosyl-L–alanine with different solvent molecules were obtained by two ways of crystallization. The crystallization from water by slow evaporation of the solvent yielded crystals of modification **1**. Crystals of modification **2** were prepared by diffusion of ethanol into an aqueous solution of the tripeptide at room temperature.

Crystal structures of both modifications of Ala–Tyr–Ala have already been published based on low-order X-ray data sets ($\sin\theta/\lambda < 0.85$ Å^{-1}).[17] In order to obtain the high order reflections for water modification **1** we continued the measurement up to a resolution of $\sin\theta/\lambda = 1.24$ Å^{-1} with synchrotron radiation (beamline D3 at Hasylab/DESY, Hamburg, Germany) using a recently installed He gas stream cooling (Helijet) to allow a data collection at 9 K.‡ For **2**, intensity data was measured with Mo Kα radiation at 20 K on a Huber four circle diffractometer equipped with a double stage closed-cycle He cryostat where a 0.1 mm Kapton film vacuum chamber around the cold head was used.[32]‡ Diffracted intensities were measured with a MAR165-CCD area detector at the synchrotron beamline[33] while a Bruker APEX-CCD detector[34] was used at the Huber diffractometer. The XDS software[35] was applied for integration of the MAR detector data, while this was done with SAINT and SADABS[34] for the APEX data.

Spherical refinements of both structures **1** and **2** were performed with SHELXL[36] and the obtained spherical models were used as the input for aspherical atom multipole formalism[37] using the program package XD.[18] The hexadecapolar level of the multipole populations was used for C, N and O atoms, while bond-directed dipoles were applied for H atoms. Moreover, for the partially occupied water molecule the occupancies of O(8), H(81) and H(82) atoms were kept fixed and the multipole parameters were constrained to those of the fully-occupied water molecule: O(6), H(61) and H(62). During the final cycles of both refinements for **1** and **2**, ten κ parameters were refined in the least-squares procedure. Three-fold symmetry, *3*, was introduced for methyl carbon atoms (C7, C8, C32) and ammonium nitrogen atom (N1). Moreover, *m* symmetry was assigned to the atoms of peptide bonds (C2, N2, C4, N3), the carbon atom of carboxylate group (C6), the C atoms in phenyl ring (C21–C26) and water oxygen atoms (O6, O7, O8). The bond lengths to H atoms were set to standard neutron distances.[38]

Fig. 6a–b show the residual density maps in the planes of the peptide bond O(1)C(2)N(2) for **1** and **2**. It should be noted that for the water modification (Fig. 6a) a slightly higher noise level is observed in comparison to the ethanol one (Fig. 6b), however, no significant residual density shows up.

‡ CCDC reference numbers 609565–609566. For crystallographic data in CIF format see DOI: 10.1039/b607744g

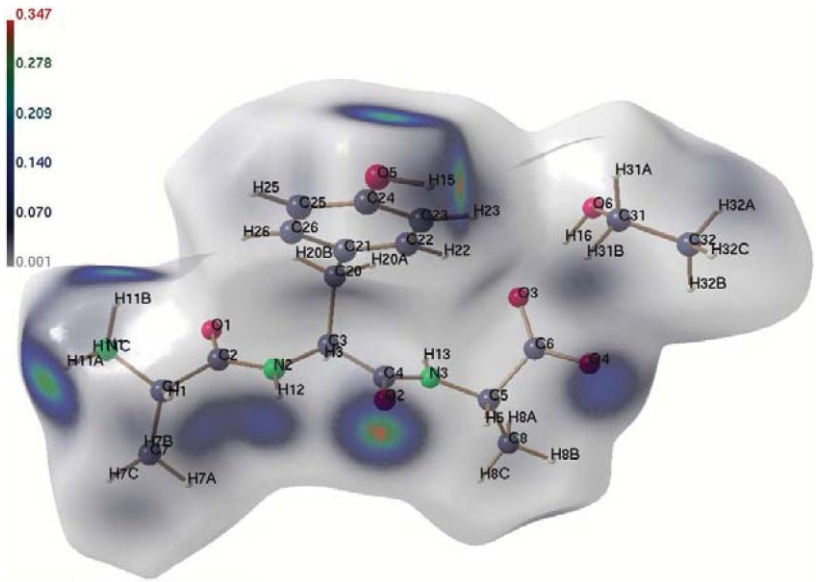

Fig. 3 Three-dimensional representation of the Hirshfeld surface for the ethanol modification **2** calculated from experimental charge density (drawing generated with Moliso[25]). Crystal electron density (e Å^{-3}) mapped by a colour code onto this surface, see colour bar.

Further details of the multipole refinements for **1** and **2** are presented in Table 6.

Theoretical calculations

To explore experimental results *versus* theory, single-point density-functional calculations were performed using the program package GAUSSIAN 03.[39] The calculations were based on the experimental geometry of **1** and **2** at the B3LYP/6-311 + + G(3df,3pd) level of approximation. Topological analysis was performed with the program AIM 2000.[40] Since the molecular geometries of **1** and **2** are very similar, the derived topological properties from these calculations agree within 0.01 e Å^{-3}/0.2 e Å^{-5} for $\rho(\mathbf{r}_{BCP})/\nabla^2\rho(\mathbf{r}_{BCP})$, so that only the theoretical means of **1** and **2** are listed in Table 1.

Conclusions

The existence of the title tripeptide L-Ala–L-Tyr–L-Ala in two crystal lattices with similar molecular structures (and even similar intermolecular interactions, in most cases) offered the favorable opportunity to examine the reproducibility of the charge density of the title molecule in different crystal structures but widely comparable crystalline environments. In addition, the experimental conditions were different, synchrotron primary radiation, open

Table 6 Crystallographic data and multipole refinement details for **1** and **2**‡

	1	**2**
Chemical formula	$C_{15}H_{21}N_3O_5 \times 2.634\ H_2O$	$C_{15}H_{21}N_3O_5 \times C_2H_5OH$
M_r	370.82	369.42
Cell setting, space group, Z	Monoclinic, $P2_1$ (no.4), $Z = 2$	Monoclinic, $P2_1$ (no.4), $Z = 2$
a, b, c/Å	8.121(4), 9.299(6), 12.532(5)	8.845(2), 9.057(2), 12.364(3)
β (deg)	91.21(2)	94.56(3)
V/Å^3	946.2(7)	987.3(3)
T/K	9	20
$\sin\theta/\lambda$/Å^{-1} or d/Å	1.24 (0.40)	1.11 (0.45)
No. of measured reflections	203534	112650
No. of unique reflections	14111	11703
Redundancy	14.4	9.6
Completeness (%)	91.2	99.4
R_{int}	0.0535	0.0415
No. of reflections (N_{ref})	12875	10901
No. of variables (N_v)	683	722
$R(F)$, $R_{all}(F)$, $R_w(F)$	0.0293, 0.0351, 0.0208	0.0223, 0.0264, 0.0177
$R(F^2)$, $R_{all}(F^2)$, $R_w(F^2)$	0.0350, 0.0364, 0.0412	0.0292, 0.0300, 0.0350
G_{of}	2.06	1.63
N_{ref}/N_v	18.8	15.1
$\Delta\rho_{min}$, $\Delta\rho_{max}$/e Å^{-3}	−0.360, 0.329	−0.235, 0.273

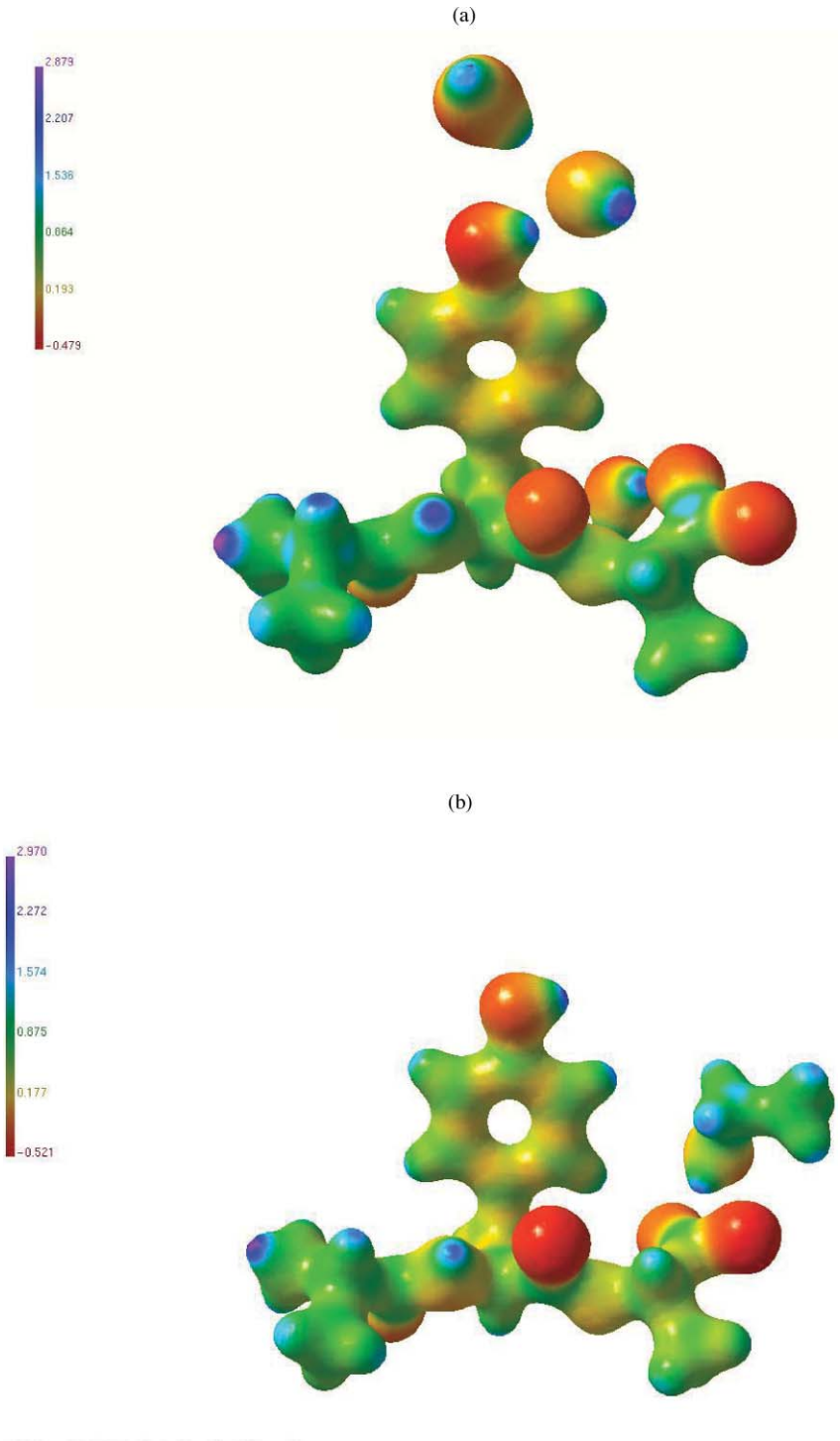

Fig. 4 Three-dimensional representation of the electrostatic potential for **1** (a) and **2** (b) calculated from the experimental charge densities (drawing generated with Moliso[25]). The colour code is shown by the colour bar.

flow He gas stream cooling, MAR165-CCD area detector for **1**; conventional Mo Kα radiation, closed cycle cryostat cooling and Bruker APEX-CCD area detector for **2**. The topological analysis of the experimental charge densities allowed a detailed quantitative comparison of both data sets and indicated a reproducibility of bond topological properties within 0.07 e $Å^{-3}$/4.9 e $Å^{-5}$ for $\rho(\mathbf{r}_{BCP})/\nabla^2\rho(\mathbf{r}_{BCP})$ and 0.8 $Å^3$ and 0.1 e for atomic volumes V_{001} and charges Q_{001}. These average uncertainties are in line with several literature studies, where quantitative data of this type were compared.

The important question of the transferability of submolecular properties was examined with respect to the reference tripeptide L-Ala–L-Ala–L-Ala. The agreement of bond and atomic topological properties is in the same range as given above for the

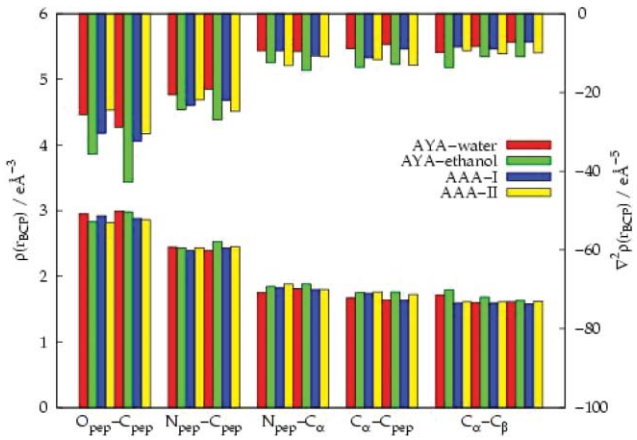

Fig. 5 Comparison of the bond topological properties of different types of bonds within the main peptide chain for L-Ala–L-Tyr–L-Ala (**1** and **2**) and L-Ala–L-Ala–L-Ala (**3**), molecules I and II derived from experiment.

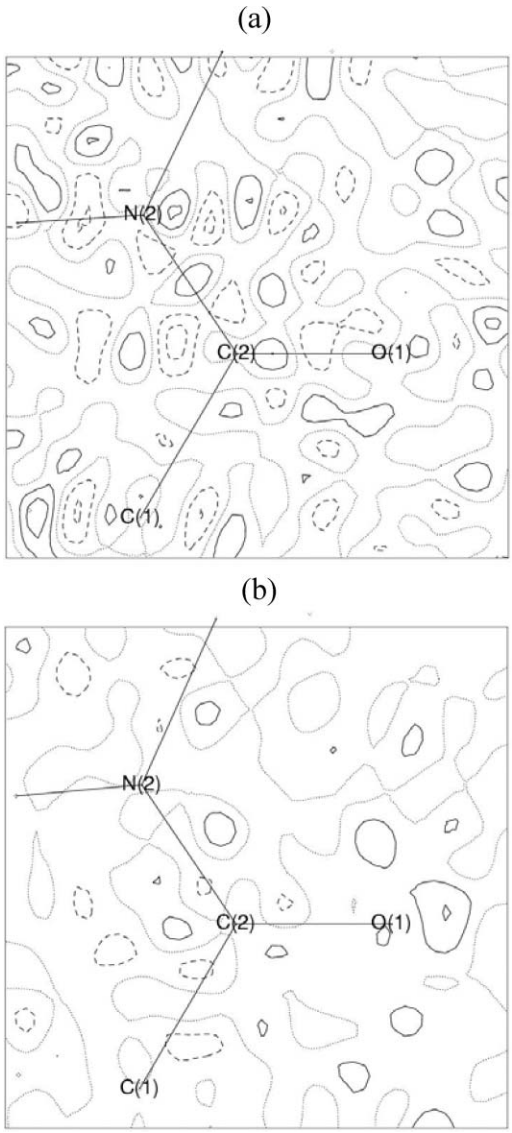

Fig. 6 Residual maps in the peptide bonds for **1** (a) and **2** (b). Positive, negative and zero contours are represented by solid, dotted and dashed lines, respectively. Contour intervals at 0.1 e Å^{-3}.

reproducibility. It follows that from the replacement of the central amino acid L-Ala by L-Tyr no influence is seen, neither on bond nor on the atomic properties. If there is any influence it is beyond the accuracy of experimental electron density work being reachable at present. These findings confirm experimentally the nearest/next nearest neighbor approximation[41] and support the use of the presently developing data base approaches for electron density modelling of polypeptides where the transferability principle is an essential prerequisite for their validity. To substantiate the present results further, more charge density studies on the system Ala-xxx-Ala are in progress so that the influence of individual amino acid residues on the topology of oligopeptide main chains can be studied on a broader basis of quantitative properties.

Acknowledgements

This work was financially supported by the Deutsche Forschungsgemeinschaft (DFG) (grant Lu 222/27-1).

References

1 P. Coppens, *Angew. Chem.*, 2005, **117**, 6970–6972.
2 P. Luger, A. Wagner, Ch. B. Hübschle and S. I. Troyanov, *J. Phys. Chem. A*, 2005, **109**, 10177–10179.
3 R. F. W. Bader, *Atoms in Molecules—A Quantum Theory*, Clarendon Press,Oxford, U.K., 1990, p. 1994.
4 C. Gatti, R. Bianchi, R. Destro and F. Merati, *THEOCHEM*, 1992, **255**, 409–433.
5 P. Coppens, Y. Abramov, M. Carducci, B. Korjov, I. Novozhilova, C. Alhambra and M. R. Pressprich, *J. Am. Chem. Soc.*, 1999, **121**, 2585–2593.
6 R. Destro, P. Roversi, M. Barzaghi and R. E. Marsch, *J. Phys. Chem. A*, 2000, **104**, 1047–1054.
7 R. Flaig, T. Koritsánszky, B. Dittrich, A. Wagner and P. Luger, *J. Am. Chem. Soc.*, 2002, **124**, 3407–3417.
8 S. Scheins, B. Dittrich, M. Messerschmidt, C. Paulmann and P. Luger, *Acta Crystallogr., Sect. B*, 2004, **60**, 184–190.
9 W. D. Arnold, L. K. Sanders, M. T. McMahon, A. V. Volkov, G. Wu, P. Coppens, S. R. Wilson, N. Goudbout and E. Oldfield, *J. Am. Chem. Soc.*, 2000, **122**, 4708–4717.
10 S. Mebs, M. Messerschmidt and P. Luger, *Z. Kristallogr.*, 2006, DOI: 10.1524/zkri.2006.221.1.
11 C. F. Matta and R. F. W. Bader, *Proteins: Struct., Funct., Genet.*, 2000, **40**, 310–329.
12 C. F. Matta and R. F. W. Bader, *Proteins: Struct., Funct., Genet.*, 2002, **48**, 519–538.
13 C. F. Matta and R. F. W. Bader, *Proteins: Struct., Funct., Genet.*, 2003, **52**, 360–399.
14 B. Dittrich, T. Koritsánszky, M. Grosche, W. Scherer, R. Flaig, A. Wagner, H.-G. Krane, H. Kessler, C. Riemer, A. M. M. Schreurs and P. Luger, *Acta Crystallogr., Sect. B*, 2002, **58**, 721–727.
15 M. Messerschmidt, S. Scheins and P. Luger, *Acta Crystallogr., Sect. B*, 2005, **61**, 115–121.
16 E. Rödel, M. Messerschmidt, B. Dittrich and P. Luger, *Org. Biomol. Chem.*, 2006, **4**, 475–481.
17 L. Chęcińska, D. Förster, W. Morgenroth and P. Luger, *Acta Crystallogr., Sect. C*, 2006, **62**, 454–457.
18 T. Koritsánszky, P. R. Mallinson, S. T. Howard, A. Volkov, P. Macchi, Z. Su, C. Gatti, T. Richter, L. J. Farrugia and N. K. Hansen, *XD–A Computer Program package for Multipole Refinement and Analysis of Electron Densities from Diffraction Data*, 2003.
19 A. Volkov, Y. Abramow, P. Coppens and C. Gatti, *Acta Crystallogr., Sect. A*, 2000, **56**, 332–339.
20 A. Volkov, C. Gatti, Y. Abramow and P. Coppens, *Acta Crystallogr.. Sect. A*, 2000, **56**, 252–258.
21 U. Koch and P. L. A. Popelier, *J. Phys. Chem.*, 1995, **99**, 9747–9754.

22 E. Espinosa, E. Molins and C. Lecomte, *Chem. Phys. Lett*, 1998, **285**, 170–173.
23 E. Espinosa, M. Souhassou, H. Lachekar and C. Lecomte, *Acta Crystallogr., Sect. B*, 1999, **55**, 563–572.
24 J. J. McKinnon, A. S. Mitchell and M. A. Spackman, *Chem.—Eur. J.*, 1998, **4**, 2136–2141.
25 Ch. B. Hübschle, *MOLISO. A Program for Color Mapped Isosurfaces*, Free University of Berlin, 2005.
26 Z. Su and P. Coppens, *Acta Crystallogr., Sect. A*, 1992, **48**, 188–197.
27 B. Dittrich, *Herleitung Atomarer Eigenschaften von Oligopeptiden aus ihren Experimentellen Elektronendichten*, 2002, PhD thesis, Freie Universität Berlin, Berlin, Germany.
28 V. Pichon-Pesme, C. Lecomte and H. Lachekar, *J. Phys. Chem. B.*, 1995, **99**, 6242–6250.
29 A. Volkov, X. Li, T. Koritsánszky and P. Coppens, *J. Phys. Chem. A.*, 2004, **108**, 4283–4300.
30 B. Dittrich, T. Koritsánszky and P. Luger, *Angew. Chem., Int. Ed.*, 2004, **43**, 2718–2721.
31 B. Dittrich, Ch. B. Hübschle, M. Messerschmidt, R. Kalinowski, D. Girnt and P. Luger, *Acta Crystallogr., Sect. A*, 2005, **61**, 314–320.
32 M. Messerschmidt, M. Meyer and P. Luger, *J. Appl. Crystallogr.*, 2003, **36**, 1452–1454.
33 C. Paulmann and W. Morgenroth, *HASYLAB Annual Report*, 2005, 1121–1122.
34 Bruker AXS Inc. programs *ASTRO, SMART, SAINT, SADABS*, Bruker AXS Inc.,Madison, Wisconsin, USA, 1997–2001.
35 W. Kabsch, *J. Appl. Crystallogr.*, 1993, **26**, 795.
36 G. M. Sheldrick, *SHELXS-97, Program for solution of crystal structures*, University of Göttingen, Germany, 1997; G. M. Sheldrick, *SHELXL-97, Program for refinement of crystal structures*, University of Göttingen, Germany, 1997.
37 N. K. Hansen and P. Coppens, *Acta Crystallogr., Sect. A*, 1978, **34**, 909–921.
38 F. H. Allen, O. Kennard, D. Watson, L. Brammer, A. Orpen and R. Taylor, *International Tables of Crystallography, vol. C*, 1992, ch. 9.5, pp. 685–706, Kluwer Academic Publishers, Dordrecht.
39 M. J. Frisch, G. W. Trucks, H. B. Schlegel, G. E. Scuseria, M. A. Robb, J. R. Cheeseman, J. A. Montgomery, Jr., T. Vreven, K. N. Kudin, J. C. Burant, J. M. Millam, S. S. Iyengar, J. Tomasi, V. Barone, B. Mennucci, M. Cossi, G. Scalmani, N. Rega, G. A. Petersson, H. Nakatsuji, M. Hada, M. Ehara, K. Toyota, R. Fukuda, J. Hasegawa, M. Ishida, T. Nakajima, Y. Honda, O. Kitao, H. Nakai, M. Klene, X. Li, J. E. Knox, H. P. Hratchian, J. B. Cross, C. Adamo, J. Jaramillo, R. Gomperts, R. E. Stratmann, O. Yazyev, A. J. Austin, R. Cammi, C. Pomelli, J. W. Ochterski, P. Y. Ayala, K. Morokuma, G. A. Voth, P. Salvador, J. J. Dannenberg, V. G. Zakrzewski, S. Dapprich, A. D. Daniels, M. C. Strain, O. Farkas, D. K. Malick, A. D. Rabuck, K. Raghavachari, J. B. Foresman, J. V. Ortiz, Q. Cui, A. G. Baboul, S. Clifford, J. Cioslowski, B. B. Stefanov, G. Liu, A. Liashenko, P. Piskorz, I. Komaromi, R. L. Martin, D. J. Fox, T. Keith, M. A. Al-Laham, C. Y. Peng, A. Nanayakkara, M. Challacombe, P. M. W. Gill, B. Johnson, W. Chen, M. W. Wong, C. Gonzalez and J. A. Pople, *GAUSSIAN 03 (Revision B.04)*, Gaussian, Inc., Pittsburgh PA, 2003.
40 F. Biegler-König, *AIM 2000*, University of Applied Sciences, Bielefeld, Germany, 2000.
41 T. Koritsánszky, A. Volkov and P. Coppens, *Acta Crystallogr., Sect. A*, 2002, **58**, 464–472.
42 A. L. Spek, *J. Appl. Crystallogr.*, 2003, **36**, 7–13.